

FRACTAL MEASUREMENT AND LINE GENERALIZATION

PAUL A. LONGLEY and MICHAEL BATTY

Department of Town Planning, University of Wales at Cardiff, P.O. Box 906, Cardiff CF1 3YN, U.K.

(Received 30 July 1987; accepted 4 July 1988)

Abstract—This paper describes a standard linear regression formulation through which the fractal dimension of cartographic lines may be ascertained. Four different algorithms for measuring the fractal character of lines are introduced: these are termed the structured walk, equipaced polygon, hybrid walk, and cell-count methods. The relative merits of these four methods are assessed using a digitized database which depicts the town of Cardiff's (U.K.) urban growth during the period 1886–1949. A concluding section assesses the methodological and substantive rationales for this measurement task.

Key Words: Fractal measurement, Line generalization, Structured walk, Equipaced polygon, Hybrid walk, Cell count.

1. INTRODUCTION

Fractal concepts now are being used in many areas of scientific enquiry and two complementary approaches can be identified. First, the description of irregularity in a formal framework has led to the application of fractals in many traditional areas of scientific *measurement* which are being informed by these ideas. Second, complementing description and measurement is the notion that fractals can be used to generate or *simulate* irregularity by building computer models of various natural and artificial forms. Indeed, it has been argued that the use of computer graphics in visualizing fractal concepts has played a central part in popularizing these ideas, and this is clearly the situation in mathematics where abstract notions of space have been visualized in entirely new ways through the convergence of fractals and computer graphics. The power of these concepts has been illustrated further through their commercial exploitation in the computer-graphics industry. In the spatial sciences, particular attention has been focused on the way in which fractals may be used to generate visually realistic simulations of a variety of natural and man-made phenomena such as cartographic features encountered in geographical enquiry (Batty, 1985; Goodchild and Mark, 1987). This paper takes a step backwards from the practice of *generating* or *simulating* cartographic lines as fractal forms and reviews a number of ways in which the fractal dimension ("fractality") of such lines may be *measured*.

A three-fold rationale for this exercise may be outlined. First, in an era in which map management (either as an end in itself or as a component of geographical information systems) increasingly involves storage of digitized data in computer-readable form, the question arises as to what is the most appropriate number and spacing of points for efficient storage and effective display. An emerging consensus (e.g. Muller, 1987; Buttenfield, 1984) suggests that fractals provide

more visually acceptable models of total line character than other more established methods based upon prespecified point weeding intervals or band-width tolerancing. Second, there also is increasing support for the notion that fractals offer a panacea for cartographic line simulation in a variety of contexts. Although plausible levels of visual realism have been produced in some existing simulations (Batty and Longley, 1986), the increased sophistication of such computer graphic simulations (and of the devices on which they are displayed) is likely to require the specification of empirical fractal dimensions about which statistical fractals are to be measured and associated simulations generated. The measurement task should necessarily precede large-scale simulation in such instances. The third, and in the present example most controversial, rationale for fractal measurement surrounds its role in enhancing our understanding of the various processes which conspire to produce a final cartographic delineation on a map. Fractals have been used in various natural scientific domains (e.g. Clark, 1986; Dearnley, 1985; Kaye, Leblanc, and Abbot, 1985; Schertzer and Lovejoy, 1984) to infer the effects of a single process (or a small number of different processes). In moving from objective measurement of a distinct physical boundary to subjective cartographic representation of altogether different geographical phenomena, inference from form to process inevitably becomes incalculably more difficult and controversial. Insofar as these processes may be more manifold, multifaceted, complex, and rapidly changing, fractal measurement may offer at best only a "black box" synthesis of line character: nevertheless substantive interpretations in the literature (e.g. Longley and Batty, 1989), remain sufficiently plausible to suggest that this approach should not be dismissed out-of-hand.

For present purposes, however, fractal measurement may be viewed as an end in itself. That is to say, the measurement procedure allows us to do two things: first, to diagnose whether a particular curve is

fractal and to identify the range of scales through which the fractal property of self-similarity holds; and, secondly, to assess whether the self-similarity property is exact statistically through the entire range of scales for which the fractal property has been identified. If self-similarity does not seem to be exact across the entire scale range, we may seek to accommodate this in our recorded measurements of fractal dimensions.

The remainder of this paper is structured as follows. Section 2 defines what a fractal line is and shows how fractal dimensionality can be identified as a parameter in a regression model; Section 3 addressed the empirical measurement problem; Section 4 introduces four methods of obtaining measurements and illustrates each method using a number of cartographic displays of an empirical case study; and Section 5 discusses the measurements obtained from that study, assesses the applicability of the techniques, and draws some conclusions as to future research.

2. EMPIRICAL DIAGNOSIS OF FRACTAL FORM

The central concepts underlying fractals research are the properties of indeterminate scale measure such as length, scale-dependence and self-dependence, and self-similarity (which may be exact or statistical) (Goodchild and Mark, 1987). Early research on fractal measurement (e.g. Richardson, 1961) detected the property of increasing curve length at finer and finer levels of resolution by setting a pair of dividers at a succession of spans and for each span, "walking" the dividers along the curve, and recording the number of steps that were needed to traverse its entirety. This is a neat method of illustrating the property of scale-dependent length, for adjusting the dividers to smaller and smaller spans is equivalent to focusing at finer and finer levels of resolution.

Figure 1 illustrates how this results in approximations which are tuned increasingly finely to the path of a base curve. In the top diagram, $n_0 = 5$ complete

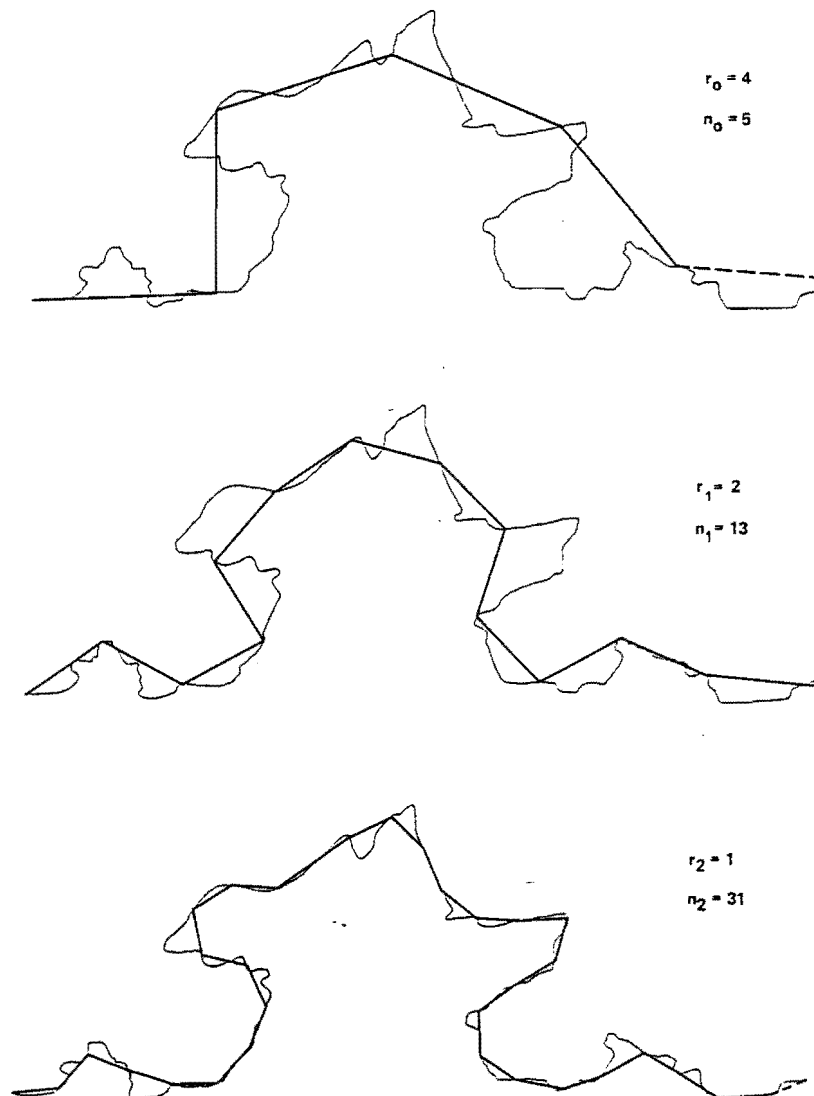


Figure 1. Measuring line length at three adjacent scales.

chords are needed to approximate the curve at divider width (scale of resolution) r_j . Changing the divider width to r_{j+1} in the middle diagram, such that $r_{j+1} = \frac{1}{2}(r_j)$, we determine that $n_{j+1} = 13$ chords are required. Thus

$$\frac{r_j}{r_{j+1}} = 2, \text{ but } \frac{n_{j+1}}{n_j} > 2. \quad (1)$$

Halving the divider width once again in the lower diagram requires 31 complete chords to traverse the curve, and we see that the same property holds. A property of a fractal line is that halving the step interval (or doubling the scale of resolution) in this way will dictate that more than twice as many steps will be needed to approximate the line. This is because increasing amounts of self-similar detail will be detected. Denoting the perimeters of the three curves $P_j (= n_j r_j)$, $P_{j+1} (= n_{j+1} r_{j+1})$, and $P_{j+2} (= n_{j+2} r_{j+2})$, it also is clear from Equation (1) that $P_{j+2} > P_{j+1} > P_j$.

For a curve which is either a pure or statistical fractal we can generalize this relationship by assuming that the ratio of the number of chord sizes at any two scales is in constant relation to the ratio of the lengths of the chords. Thus

$$\frac{n_{j+1}}{n_j} = \left[\frac{r_j}{r_{j+1}} \right]^D \cdot 1 \leq D \leq 2. \quad (2)$$

where D is the fractal dimension common to the two measurement scales. For the present, it is assumed that the fractal dimension D is invariant to scale changes, although this assumption will be reconsidered in the empirical discussion. The limits specified in Equation (2) define the special situations of a Euclidean straightline ($D = 1$, i.e. halving the scale yields exactly twice the number of chords) and a two-dimensional plane ($D = 2$, i.e. halving the scale yields four times the number of chords and the line encloses the space). Thus each of the curves which will be analyzed in Section 3 can be thought of as filling more space than a (one-dimensional) straightline, but less space than a (two-dimensional) surface.

Rearranging Equation (2) in a form suitable for statistical prediction yields:

$$n_{j+1} = (n_j r_j^D) r_{j+1}^{-D} = a r_{j+1}^{-D}, \quad (3)$$

where $n_j r_j^D$ acts as a base constant a against which the number of chords n_{j+1} from any interval size r_{j+1} may be predicted. Thus Equation (3) can be generalized easily as

$$n = a r^{-D}. \quad (4)$$

With two scales of resolution, D can be derived by rearranging Equation (2) as

$$D = \log(n_{j+1}/n_j) / \log(r_j/r_{j+1}). \quad (5)$$

However, confirmation that a common fractal dimension D holds across a wider range of scales requires

that a range of r and corresponding n values be considered. Taking logarithms of Equation (4) yields

$$\log n = \log a - D \log r. \quad (6)$$

The range of r and corresponding n values can be substituted into Equation (6) and the value of D evaluated using a simple linear regression procedure. A related equation is based upon the perimeter length P . From Equation (4):

$$P = nr = ar^{(1-D)} \quad (7)$$

and, by taking logarithms of (7):

$$\log P = \log a + (1 - D) \log r. \quad (8)$$

Obviously D also can be obtained from Equation (8) using simple regression. Equation (8) will be used in the following empirical analysis, because it allows the most appropriate way of checking the range of scales used.

3. EMPIRICAL MEASUREMENT OF FRACTAL CURVES

This section outlines four different methods of ascertaining the fractal dimension of a curve. Four corresponding algorithms were derived in order to obtain values of perimeter and step lengths which substitute into Equation (8); modifications to these algorithms and harnessing them to a graphical display device also allows pedagogic illustration of the scale-dependent measurement process.

Each of these algorithms was applied to the digitized urban boundaries of Cardiff, Wales in 1886, 1901, 1922, and 1949 (Fig. 2). These boundaries were digitized using the in-house MicroPLOT software suite (Bracken, 1985). The substantive and methodological rationale for the selection of this example might be summarized as follows. The period spanned by these time slices bounds the period of Cardiff's most rapid growth, which was consequent upon the opening up of the South Wales coalfields through railroad construction and the attendant focusing of coal exports upon the new dock facilities of Cardiff. In fact, the failure to develop the extensive industrial multipliers characteristic of some other mining areas led to the relative decline of the city in the post World War I period. At the intraurban scale, the development of the Cardiff tramway system during the late 19th and early 20th centuries promoted suburban expansion upon newly opened up tracts of land (see Daunton, 1977 for a full discussion). The period from 1860 to World War I thus represents the period of Cardiff's fastest population growth and most rapid industrial change, unsurpassed perhaps even by the development of Cardiff as the Welsh capital in the post-World War II period.

Cartographic line representation is an inherently subjective process, and the delineation of a (fast-

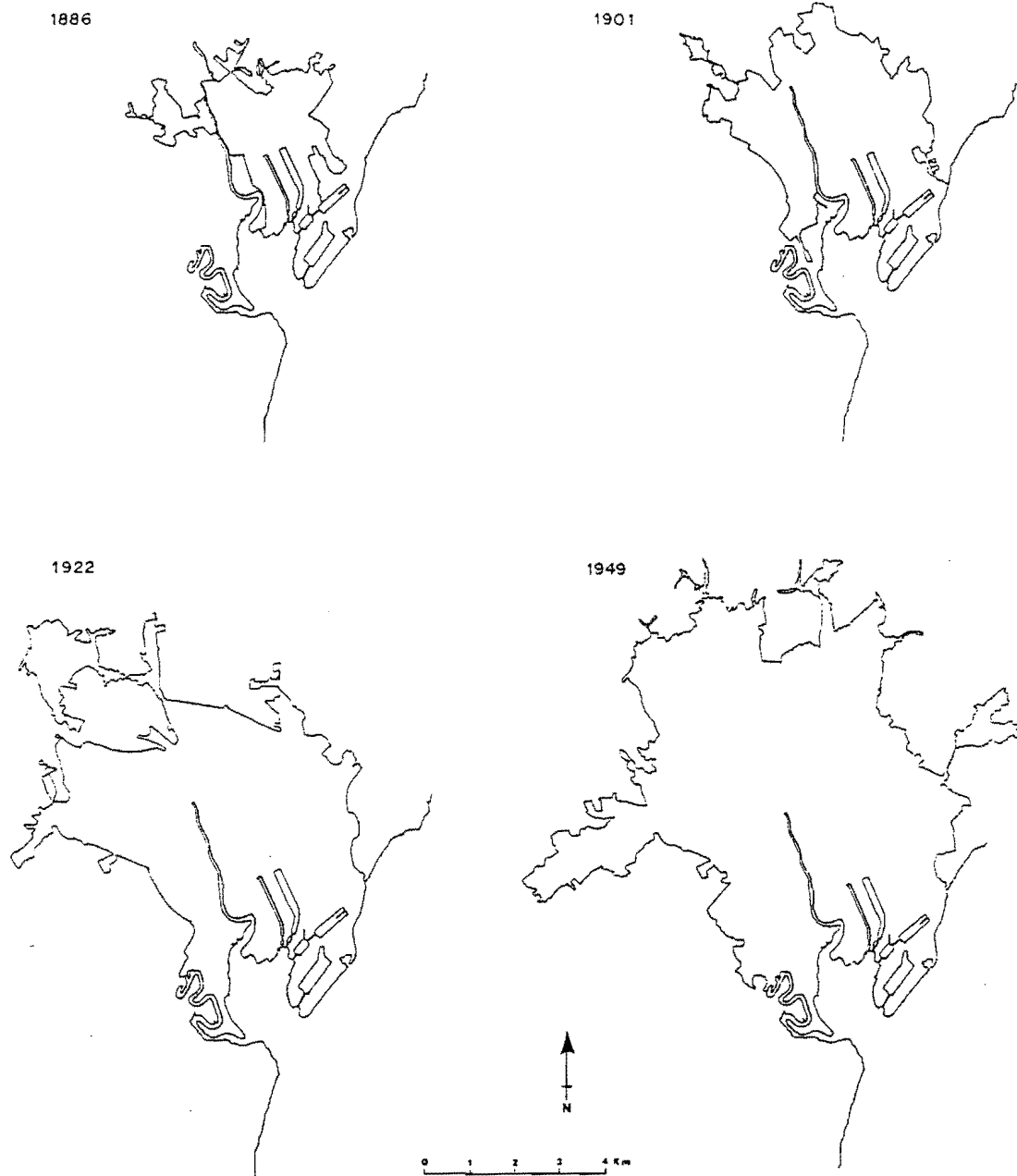


Figure 2. Digitized urban boundaries of Cardiff in 1886, 1901, 1922, and 1949.

changing and ephemeral) feature of historical urban growth inevitably tests cartographic codification conventions to the limits. In the situation of Cardiff's urban edge, decisions about the representation of "urban" allotments, the classification of disused railway sidings and the assimilation of "inliers" of rural land-use within the urban fabric posed particularly daunting problems. Fractal measurement in natural science has been applied to edges whose form are the direct consequence of a single, or only a very few, physical processes. In moving into the human domain, a similar presupposition does not hold, for an urban edge is clearly the spatial expression of a myriad of different social and economic factors which in

many instances evade precise quantification. Nevertheless, this is not to say that we cannot envisage urban phenomena as being fractal in structure; neighborhoods, shopping centers, the spatial distribution of industry and public open space, and the juxtaposition of suburbs themselves exhibit self-similarity at a variety of scales, and it is intuitively plausible to suggest that this should result in spatial expression in fractal measurements.

The central questions are, first, whether the combined effects of different urban processes find spatial expression in a fractal form, given also that delineation of this form mainly is the result of a human judgemental process; and, secondly, whether the self-

similarity consequent upon the organization of a wide range of urban phenomena manifests itself as a single unchanging fractal index. As such, this paper investigates previous findings that curves exhibit statistical fractal properties only over a limited scale range, and extends them by countenancing functional changes in the nature of fractal shapes over the widest possible scale range.

In empirical terms, statistical fractals can be diagnosed by plotting the log of scale of resolution (step length) against the log of the associated perimeter length at this scale. This standard display is known as a Richardson Plot (after Richardson, 1961). Fitting a best-fit regression line through this scatter of points yields the fractal dimension D in accordance with Equation (8). Assessment of whether the curve statistically is fractal requires judgement as to how closely the log-linear functional form established through regression fits the scatter of points. Values of R^2 will be expected to be high. Muller (1987) uses a threshold of 0.95, in view of the generally low number of fitted points and the high precision of the measurement estimates: it should be stressed (following Shelberg, Moellering, and Lam, 1982) that in this context R^2 is used in a descriptive rather than inferential sense.

It should be noted that ordinary least-squares regression estimates will be most reliable when the given number of observations is scaled at more-or-less equal intervals along the axes of the scatterplots, because the observations then approximately are weighted equally. Previous empirical studies have invoked rules-of-thumb in order to specify a range through which scale changes are likely to detect meaningful changes in corresponding curve perimeters. At the lower end of the scale range spectrum, the finest scale clearly will be dependent upon the level of resolution at which the base-level curve was digitized. Previous research (Batty and Longley, 1987) suggests an appropriate lower limit to be approximately equal to the mean length of the chords which comprise the curve, whereas an upper limit is a scale which approximates the curve with no less than eight chords. In the empirical measurement exercise outlined here, about 30 changes of scale are interpolated within these limits in accordance with a geometric criterion. In fact, measurements at or close to the upper limit frequently depend upon the starting point used to begin measuring the curve, because on the one hand this can determine whether near-unique large-scale features are detected at all and, on the other, rounding errors caused by closing the measured curve with an incomplete chord (or chords) will be far greater at such scales (Kaye, 1978). To minimize this problem, some writers (e.g. Kaye and Clark, 1985) have taken coarse scale measurements from a small number of different starting points, and then have averaged them to get a more stable final value. In the following empirical measurement exercises the exclusive dedication of a MicroVAX II computer to the project allowed this practice to be taken to its logical extreme, and each meas-

urement at every scale change is the average of the lengths recorded by commencing measurement from every successive point on the digitized curve.

4. MEASUREMENT METHODS: STRUCTURED WALK, EQUIPACED POLYGON, HYBRID WALK, AND CELL COUNT

4.1. The structured walk method

This is the original method used by Richardson (1961) to measure the lengths of national boundaries and coastlines. In the original application, Richardson manually walked a pair of dividers along a mapped boundary, and obtained scale-dependent measurements by adjusting the divider span. Shelberg, Moellering, and Lam (1982) first automated this procedure with an algorithm designed to approximate a digitized curve using a prespecified range of chord lengths. In the application of a similar algorithm to the Cardiff data series, the initial (base) scale level for each curve was computed by first calculating the distances between each adjacent pair of (x,y) coordinates i and $(i+1)$ using:

$$d_{i,i+1} = [(x_i - x_{i+1})^2 + (y_i - y_{i+1})^2]^{1/2},$$

$$i = 1, \dots, N - 1. \quad (9)$$

The perimeter of each base curve is given by

$$P = \sum_{i=1}^{N-1} d_{i,i+1}. \quad (10)$$

The initial scale level for each chord was taken to be the average chord length, that is

$$r_j = P/(N - 1). \quad (11)$$

In practice the upper limit of a minimum of eight or so chords was met by basing the scale changes on the progression $r_k = 2^k r_j$, $k = 1, 2, \dots, 31$. This gave 30 changes in scale which conformed to the criteria identified. In fact, this sequence of scale adjustments was used to gauge the effect of scale change using each of the four different measurement methods, although strictly speaking the use of the mean digitizing interval is of less direct relevance in the initiation of the cell-count progression.

The walk at any given scale begins by calculating the distance $d_{p,i}$ from a starting point (x_p, y_p) to the second coordinate pair (x_i, y_i) using Equation (9). If this distance is less than the chord length, r , the next coordinate pair (x_{i+1}, y_{i+1}) is selected, the distance $d_{p,i+1}$ is computed and the test against chord length r is made again. This process continues until the distance $d_{p,i+k} > r$ and when this is achieved, a new point $[x_{p+1}, y_{p+1}]$ is interpolated onto the line segment which joins points $[x_{i+k-1}, y_{i+k-1}]$ and $[x_{i+k}, y_{i+k}]$. The walk then recommences from this interpolated point and proceeds through painstaking use of trigonometry to span the curve with chords of exactly length r . As the end of the curve is approached, the distance between the last interpolated point and the

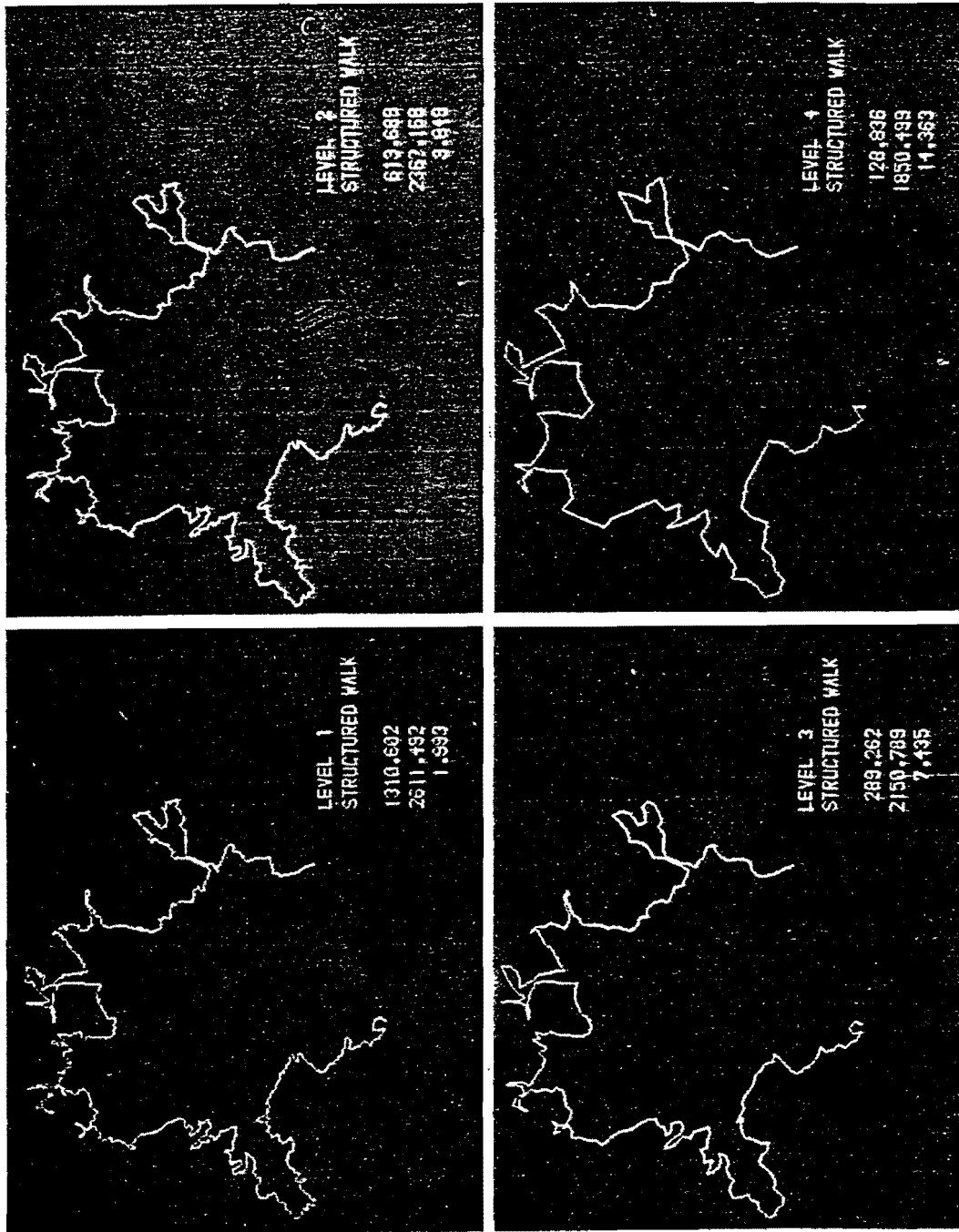


Figure 3. Illustration of structured walk procedure, using interactive computer graphics displays.

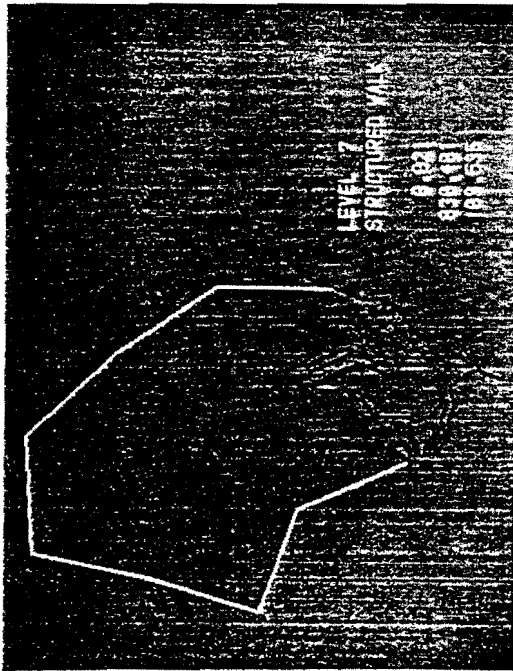
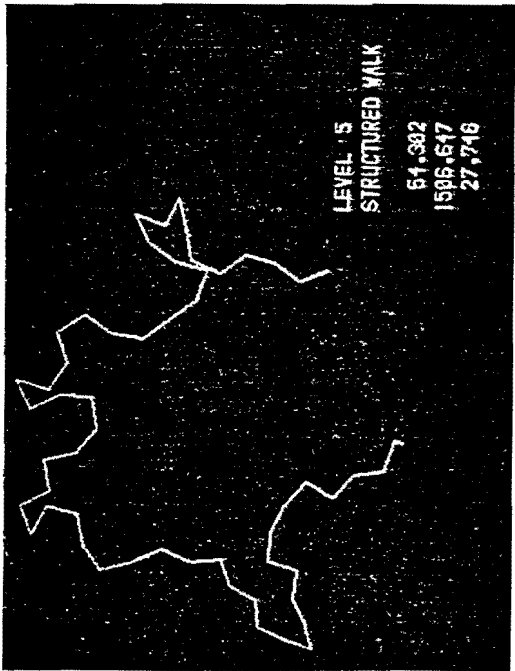
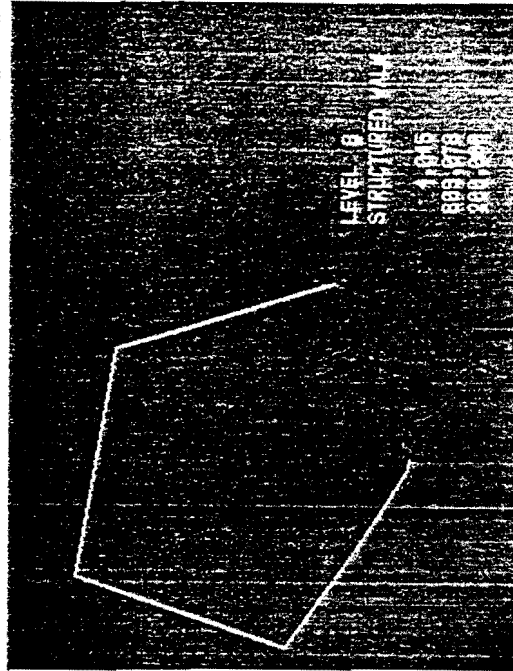
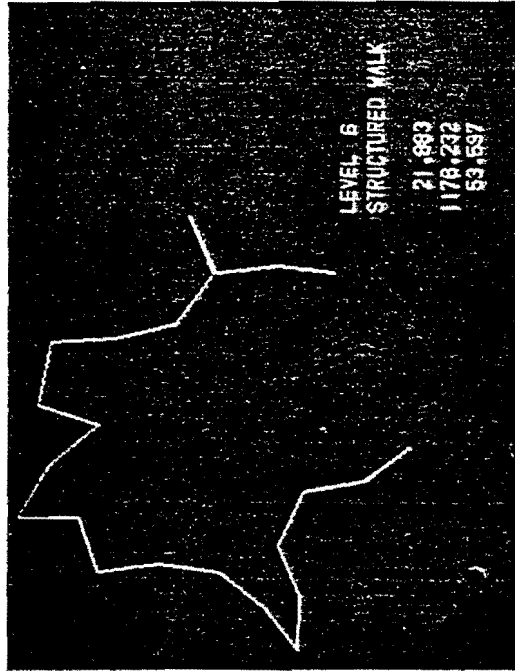


Figure 3. (Continued)

end point almost will invariably be less than r ; in this instance, a fraction of the chord length r is computed in order to close the interpolated curve. Measured perimeter (P) lengths at any scale (r) can be obtained from any starting point on the digitized base curve; if the walk begins other than at either of the end points, the interpolation proceeds along the curve in both directions and the final recorded length comprises the sum of these computations. As stated previously, the empirical measurements recorded in the Cardiff exercise comprise the average of the lengths measured from every possible starting point on the curve, repeated, of course, for every scale change.

The rudiments of this procedure are given visual expression in Figure 3. These displays of the 1949 Cardiff urban edge were produced using an interactive version of the structured walk algorithm, in which the operator specifies the initial and final chord lengths (the former as a percentage of mean chord length on the base curve, the latter as an absolute value), the starting point on the base curve, and the number of generalizations (levels) that are to be produced using the walk algorithm. Screen annotation for each level records (from bottom to top) the chord length to be

interpolated onto the base curve, the measured perimeter of the curve at this scale, and the number (complete or partial) traverses that are necessary to close the curve on its endpoints. The sequence of displays allows the operator to gain a visual appreciation of the manner in which measured perimeter lengths (and number of chords) decrease as scale increases, and could also assist a decision on the level of fractal detail most appropriate to the storage and display of a given digitized data set.

The results of the full 30 scale-change interpolations over the four time periods are presented as Richardson Plots in Figure 4. What becomes immediately apparent is that the scatter of points does not follow the straightline trend which would have indicated that the log-linear regression of Equation (8) summarized adequately the trend in the data. Rather, some other functional form seems to be required. Previous research has pointed out that fractal concepts only can be applied usefully across a restricted range of scales which are unique to a particular phenomenon under study. Other research has highlighted apparent discontinuities in the Richardson Plots (e.g. Nakano, 1984; Schertzer and Lovejoy

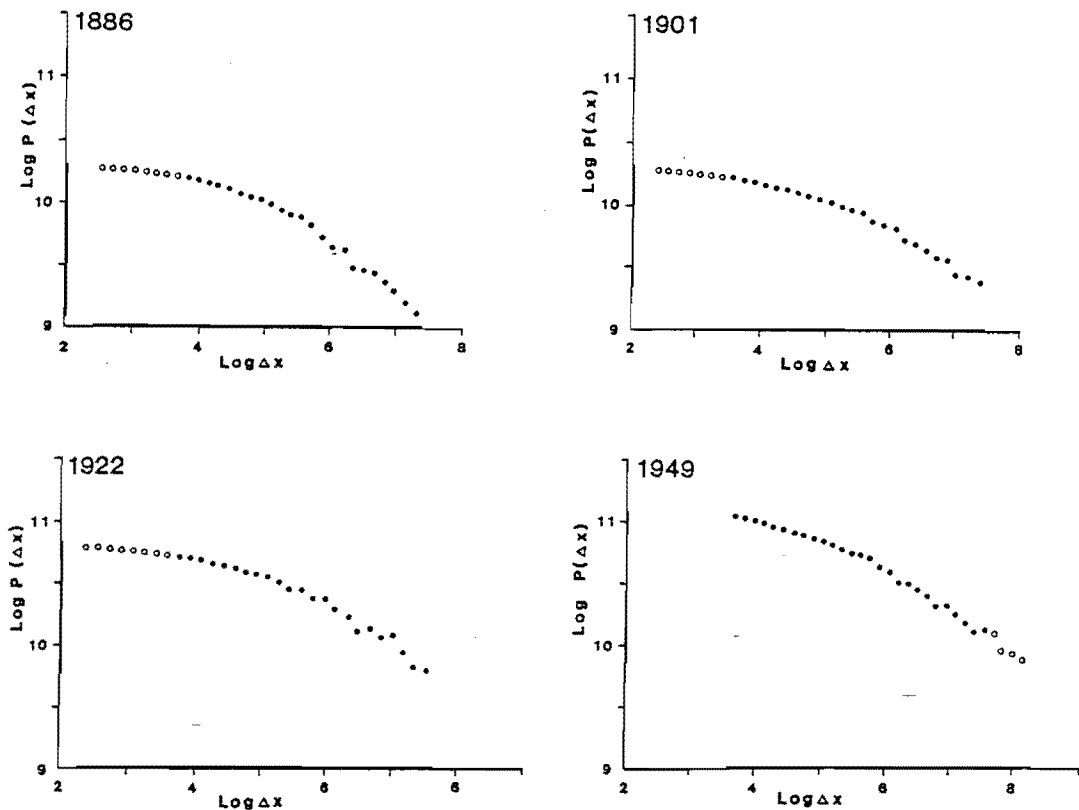


Figure 4. Richardson Plots of perimeter-scale relations for four time slices: structured walk method. Base curve data were digitized using historical maps of different scales and thus substantive interpretation of these results can concern only the common scale range observations which are represented by solid circles in Figures 4, 6, 7, and 9 (Longley and Batty, 1989). In view of primarily methodological focus to this paper, this distinction between common scale range and other observations is not made for purposes of regression analyses which follow. ● — Denotes observation falling within scale range common to all line slices.

Table 1. Structured walk method: computational costs and statistical performances of competing functional forms

Date	CPU usage Days: hours: minutes	Log-Linear form (8)			Transient dimension model (12)			
		Log a	D	R ²	Log a	d*	b ₂ × 10 ⁻⁵	R ²
1886	15:23	11.080	1.239	0.914	10.719	1.141	5.865	0.983
1901	19:11	10.886	1.184	0.927	10.622	1.117	3.947	0.985
1922	2:07:10	11.393	1.186	0.907	11.114	1.109	3.901	0.984
1949	7:49	12.150	1.267	0.975	11.883	1.211	1.202	0.991

* $d = 1 + b_1$ (when $r = 0$)

1984) and has applied separate regressions to the observations lying to the left and to the right of these points. An interesting feature of Figure 4, which perhaps arises from the use of a large number of observations in this study, is that the Richardson Plots each imply a single continuous curvilinear functional form, rather than an amalgam of juxtaposed log-linear forms. In effect it is not possible to identify clear breaks in the slopes of the plots, and thus the fitting of any number of log-linear functions to the data would remain arbitrary.

Experimentation with a number of different regression lines led to the selection of

$$\log P = \log a - b_1 \log r - b_2 r \log r \quad (12)$$

as the best statistical fit. The goodness-of-fit (R^2) of this form compared to that specified in Equation (8) is presented in Table 1. The interpretation of Equation (12) is that the fractal dimension itself is a function of scale and that the scaling coefficient ($1 - D$) is given by

$$(1 - D) = b_1 + b_2 r. \quad (13)$$

As the scale $r \rightarrow 0$ in Equation (12), so $D \rightarrow 1 - b_1$. As such, the term $b_2 r \log r$ in Equation (12) acts as a dispersion factor which increases the fractal dimension at increased scales [Eq. (12) reduces to Eq. (8) when $b_2 = 0$]. This form is referred to as the transient dimension model.

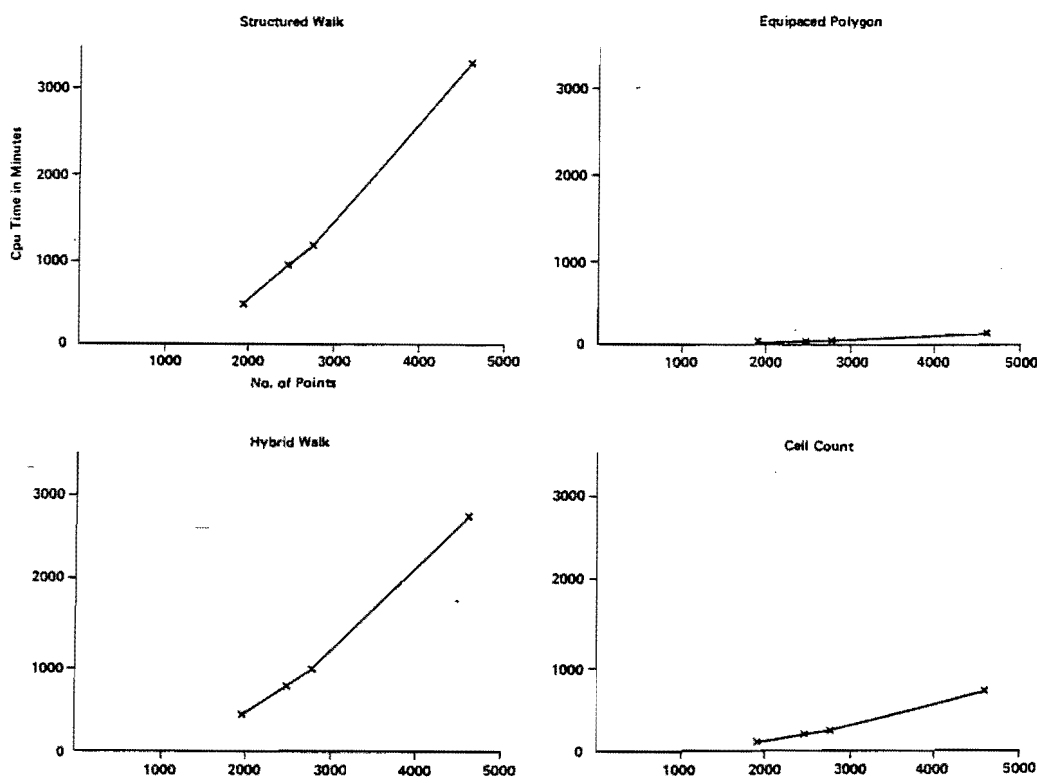


Figure 5. CPU usage of four measurement methods.

The R^2 values presented in Table 1 suggest that the transient dimension model Equation (12) produces a consistently better statistical fit than the standard log-linear form for every one of the four time slices under analysis. The Richardson Plots shown in Figure 4 illustrate that the structured walk method produced estimates which correspond closely to this functional form, with the clearest continuous trend being discernible for the smaller step lengths. Although the positioning of the points does become slightly more erratic for the largest step lengths, there is no evidence of any sudden "flattening" of the curve, which would have indicated that the scales were too coarse to pick up further fractal detail. This cohesion of the larger scale points about the best fitting functional form is the result of the averaging of each scale observation through measurements from every single possible starting point. Finally Figure 5 shows that the structured walk method is associated consistently with the highest CPU usage of the four methods. This is a consequence of the precise trigonometric interpolation of points upon the base curve. It might be conjectured that this precision obviates the need to average out the measured perimeter lengths by using every conceivable starting point, although the decay in the trend in the points at larger scale steps suggests this is possibly not the situation.

4.2. The equipaced polygon method

This was first suggested by Kaye (1978) and elaborated in Kaye and Clark (1985) as a measurement method in which there is no need to compute new base-level points. The first perimeter length for the sequence of scale changes is computed by summing the distance between adjacent coordinates; the second perimeter length represents the summed distance between every second coordinate; the third sums the distance between every fourth coordinate; and so the progression continues weeding out all but every 8th, 16th, 32nd, ... etc., point. This geometric point-weeding series is contrived so as to give observations a more equal spacing in the Richardson Plots, and hence a more equal weighting in the regression analysis. In terms of the Richardson Plots and regression analysis, the chord length r in Equation (3) which is paired with an associated measured perimeter length is given by the average chord length spanning the points at the corresponding level of the point-weeding sequence.

Formally then, a direction is established from a given starting point on the baselevel curve (x_i, y_i) and a chord is constructed to a digitized point (x_{i+k}, y_{i+k}) which is k steps away from (x_i, y_i) ; k is thus an index of scale. The distance $d_{i,i+k}$ then is computed using Equation (9), and then the reset chord involving the point (x_{i+2k}, y_{i+2k}) is constructed from (x_{i+k}, y_{i+k}) . Eventually the endpoint of the baselevel curve is approached, and the level k curve is closed on this endpoint when the remaining number of base points is less than step length k (this is equivalent to the

"remainder" as described for the structured walk). Computations in both directions from the starting point are added to determine the perimeter and mean chord lengths.

The Richardson Plots associated with this method are shown in Figure 6 and the results of regression analysis in Table 2. At an intuitive level, one might anticipate that this method might yield results of a slightly more arbitrary nature, because exact perimeter lengths will be dependent upon the evenness with which the base curve has been digitized. For example, points are unlikely to have been "forced" on long straight sections, so these sections are unlikely to contain chord endpoints; moreover, the entire shape of a measured curve is likely to change if the base curve contains major irregularities or fissures which will be detected abruptly at a shift between two scale changes. In fact, the Richardson Plots show that any such effect is removed by the averaging process and the points actually follow a clearer trend than the structured walk plots. The regression results compare directly with the structured walk results, both in terms of measured fractal dimensions and the statistical fits of the two competing functional form specifications. The biggest apparent difference between the two methods seems to be CPU usage (Fig. 5 and Table 2), in that the equipaced polygon method used < 5% of the resources required by the structured walk for a fully averaged run. However, intermediate polygon plots are more erratic than structured walk ones when full averaging does not take place.

4.3. The hybrid walk method

This was suggested by Clark (1986) as a method which retains some favorable characteristics of both the structured walk and the equipaced polygon methods. It is based directly upon the same prespecified geometric chord length series as the structured walk, which makes it less vulnerable than the equipaced polygon method to the spacing of points on the base curve. However, it is similar to the equipaced polygon method in that no new points are interpolated onto the base curve; rather, each chord is either extended or contracted to coincide with the nearest digitized point, which then is used as the origin from which the next chord is sought. Removal of the time-consuming trigonometric interpolations thus serves to speed up the computations. It is based on the same lowest level of resolution (r_j) as the previous two methods and entails similar treatment of the "remainder" distance as the end of the curve is approached.

Formally, the method proceeds in the same way as the structured walk, except that when a point (x_{i+k}, y_{i+k}) is reached where $d_{p,i+k} > r$, no new point is interpolated using the Shelberg, Moellering, and Lam algorithm. If $|d_{p,i+k} - r| \leq |d_{p,i+k-1} - r|$ then point (x_{i+k}, y_{i+k}) is selected; if not, then the point (x_{i+k-1}, y_{i+k-1}) is selected, because this point is the closest to the point at which chord length r intersects the base curve.

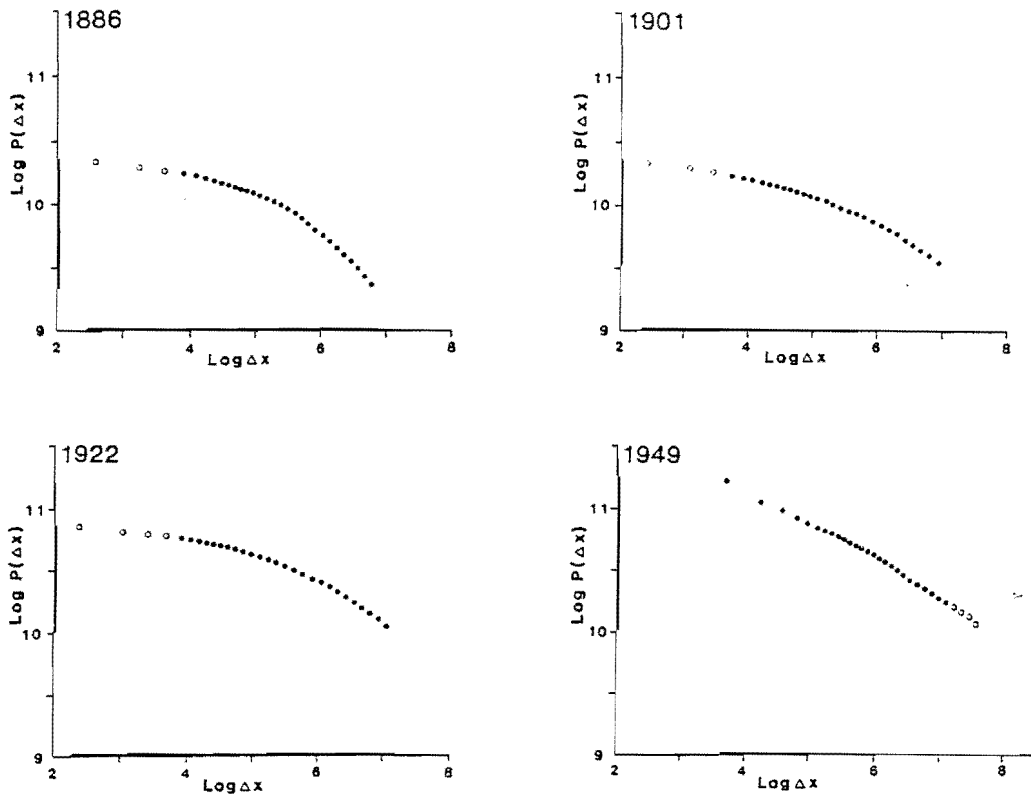


Figure 6. Richardson Plots of perimeter-scale relations for four time slices: equipaced polygon method.
 ● — Denotes observation falling within scale range common to all time slices.

The Richardson Plots associated with this method (Fig. 7) show a similar pattern to those of the structured walk method (Fig. 4). The analytical results (Table 3) also are comparable with the first two methods, although the method is unable to discriminate between the log-linear forms of the 1901 and 1922 series. The graphs of CPU usage (Fig. 5) show that only comparatively modest savings are made compared to the structured walk method, and the equipaced polygon method remains the least demanding by far in this respect.

4.4. The cell-count method

This method is more akin to a rasterized conception of the digitized base curve and has been suggested by a number of authors (Dearnley, 1985; Goodchild, 1980; Morse and others, 1985). In effect, the computer algorithm imposes a square lattice for a range of different spacings across the base curve. The spacings of the different lattices introduce the sequence of scale changes over which the irregularity of the base curve is to be measured. At each scale (grid spacing), the cell-count algorithm simply enumerates all of the cells

Table 2. Equipaced polygon method: computational costs and statistical performances of competing functional forms

Date	CPU usage Days: hours: minutes	Log-linear form (8)			Transient dimension model (12)			
		Log a	D	R ²	Log a	d*	b ₂ × 10 ⁻⁵	R ²
1886	0:36	11.176	1.236	0.875	10.589	1.086	11.200	0.995
1901	0:45	10.923	1.178	0.917	10.594	1.094	5.920	0.994
1922	2:09	11.420	1.172	0.902	11.078	1.085	5.187	0.992
1949	0:20	12.342	1.293	0.992	12.132	1.250	1.211	0.998

* d = 1+b. (when r = 0)

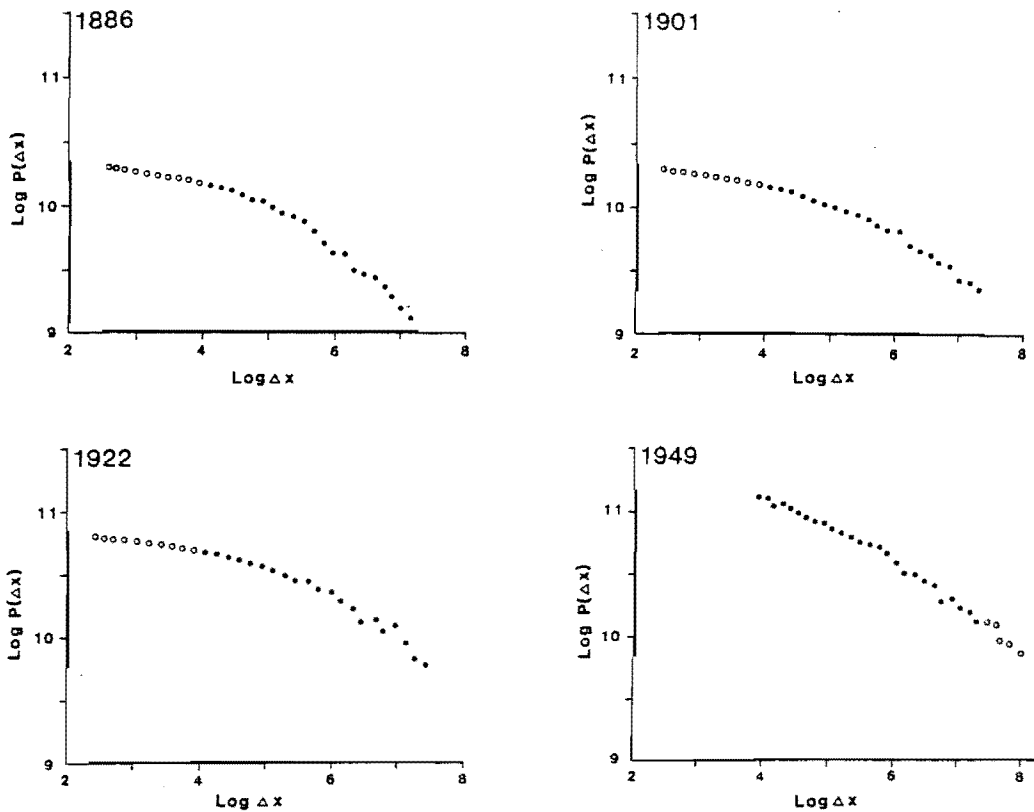


Figure 7. Richardson Plots of perimeter-scale relations for four time slices: hybrid walk method.
 ● — Denotes observation falling within scale range common to all time slices.

that the baselevel curve passes through. Counts are made at each scale change for grids originating at each point on the base curve: these are averaged to produce the final observations for each scale change in the now-familiar way. Strictly speaking, each grid scale should be defined with respect to the start and endpoints on the baselevel curve, although for reasons of convenience and comparability the empirical results reported and depicted below use the same 31 scales used for the structured and hybrid walk methods.

Formally, from a given starting point (x_p, y_p) with

a selected cell size r and direction of traverse, the next coordinate (x_i, y_i) on the base curve is alighted upon. A test is made to see if this point lies within the same square by considering whether $|x_i - x_p| \geq r$ or $|y_i - y_p| \geq r$. If either of these conditions hold, a new point is established where the coordinate in question is updated in the direction of greatest increase. Thus if $|x_i - x_p| \leq |y_i - y_p|$, $x_{p+1} = x_p + r$ and $y_{p+1} = y_p$ whilst if the converse holds, $x_{p+1} = x_p$ and $y_{p+1} = y_p + r$. If the increase along both the x and y axes is less than the grid size r , then a new coordinate point (x_{i+1}, y_{i+1}) is selected and the tests are made once again.

Table 3. Hybrid walk method: computational costs and statistical performances of competing functional forms

Date	CPU usage Days: hours: minutes	Log-linear form (8)			Transient dimension model (12)			
		Log a	D	R ²	Log a	d*	b ₂ × 10 ⁻⁵	R ²
1886	12:34	11.119	1.248	0.913	10.715	1.137	7.256	0.987
1901	15:52	10.895	1.190	0.929	10.633	1.117	4.560	0.990
1922	1:21:56	11.412	1.190	0.906	11.111	1.106	4.567	0.989
1949	6:52	12.416	1.308	0.989	12.197	1.262	1.001	0.996

* $d = 1 + b_1$ (when $r = 0$)

Each time the direction is updated, a cell has been crossed and thus is counted. Unlike the previous methods, when the endpoint of the curve is approached, the cell approximation simply finishes when the cell in which the endpoint exists has been identified.

The way in which this procedure works is illustrated in Figure 8, which shows that the intricate form of the line is lost at an early stage in the cell-count process. It is for this reason that the method has been advocated as a computationally inexpensive first approximation to measurement. Figure 5 shows that the cell-count method is closest to the equipaced polygon method in its meager CPU requirements. Although the Richardson Plots (Fig. 9) exhibit generally smooth trends, there is some evidence of "bottoming out" of the curves at the coarsest scales. This indicates that the method does not detect fractal detail at these scales, despite the averaging that has taken place. Largely because of this, the fractal dimensions and statistical fits shown in Table 4 bear less direct comparison with the other methods than has been the situation in the previous sections.

5. CONCLUSIONS

Fractal measurement presents a powerful form of cartographic line generalization which is not dependent upon a priori definition of the constituent features which make up the totality of line character. In methodological terms, such measurements might be used to manage digitized databases through selective "weeding" of those points which contribute least to overall line character; alternatively, these measurements might provide the basis to database enhancement through "rendering" of minimal digitized point information (Wise, 1987) or coarsely rasterized data.

These and other motivations have provided the impetus to the evaluation of four fractal measurement algorithms which have been assessed using numerous exploratory displays (Figs. 3 and 8) and repeatedly averaged measurements (Figs. 4, 6, 7, and 9). Repeated experimentation with the display algorithms highlighted a number of characteristics of the four methods: these include radical shifts in line approximations at adjacent order of magnitude scale changes using the equipaced polygon method, and considerable variations in coarse scale shape approximations consequent upon using different starting points in the cell-count algorithm. It seems plausible that such chance occurrences account for the moderate scattering of points about the regression trends that have been identified in some previous papers. Such chance variation can be eliminated by averaging measurements which have commenced at every single successive digitized coordinate, and it is these measurements which have been used to produce the results shown in Tables 1-4. These asymptotic results and their associated Richardson Plots show that consistent trends are detected using any of the four measurement methods, although there is some

evidence from Tables 1-4 to suggest that the cell count and hybrid walk methods are less able to detect fine trends in the data (i.e. the results show a more ambiguous trend between the 1901 and 1922 data series than is indicated by the other two methods). This may in part reflect the "bottoming out" of the Richardson Plots for coarse cell-count approximations, indicating that the cell count in particular is the least reliable of the four methods at the coarsest scales. The major difference amongst the four methods concerns central processor usage, with Figure 5 showing a measured difference between the modest requirements of the cell count and equipaced polygon methods on the one hand, and the structured walk and hybrid walk methods on the other. In practical measurement situations the choice would seem to lie between a few passes through the data using a robust but time-consuming walk method, or greater use of averaging (perhaps also across a narrower range of scale changes) using the equipaced polygon or cell-count methods.

A second important issue also arises from these empirical results, and concerns the functional form of the regression line which is fitted to the points on the Richardson Plots. With the possible exception of the 1949 data series (which were digitized at a different level of base curve resolution; see Longley and Batty, 1989, for a detailed explanation), the implied functional form is clearly curvilinear. Although some previous measurement work has created observations which do not follow a clear straight-line trend (e.g. Nakano, 1984; Schertzer and Lovejoy, 1984) this problem usually has been resolved by the insertion of a step function into the log-linear regressions. The insertion and placing of this step is clearly a subjective judgement which also is handicapped by chance scattering of the restricted number of unaveraged observations about the most plausible trend. It thus is a moot point whether extensive use of averaging of these data series, coupled with closer spacing of observations, might reveal the sort of continuous curvilinear functional form that has been identified here. This suggests that more careful analysis is required in future applications and that many existing applications should be reworked.

If this is indeed the situation and the base curves are "multifractal", then they are not fractal at all insofar as a single well-defined fractal dimension does not occur across the entire scale range. However, Mandelbrot (1984) acknowledges a generic statistical use of the term "fractal" which, firstly, allows discretion to be exercised with respect to the range of scales which are used to identify a single fractal dimension and, secondly, recognizes that many problems necessarily will involve more than a single fractal set. It is this second qualification that is of greatest importance in the present context, and one of the reasons why Mandelbrot introduces it concerns the occurrence of fractals which are embedded in spaces (and by extension of this argument, time slices)

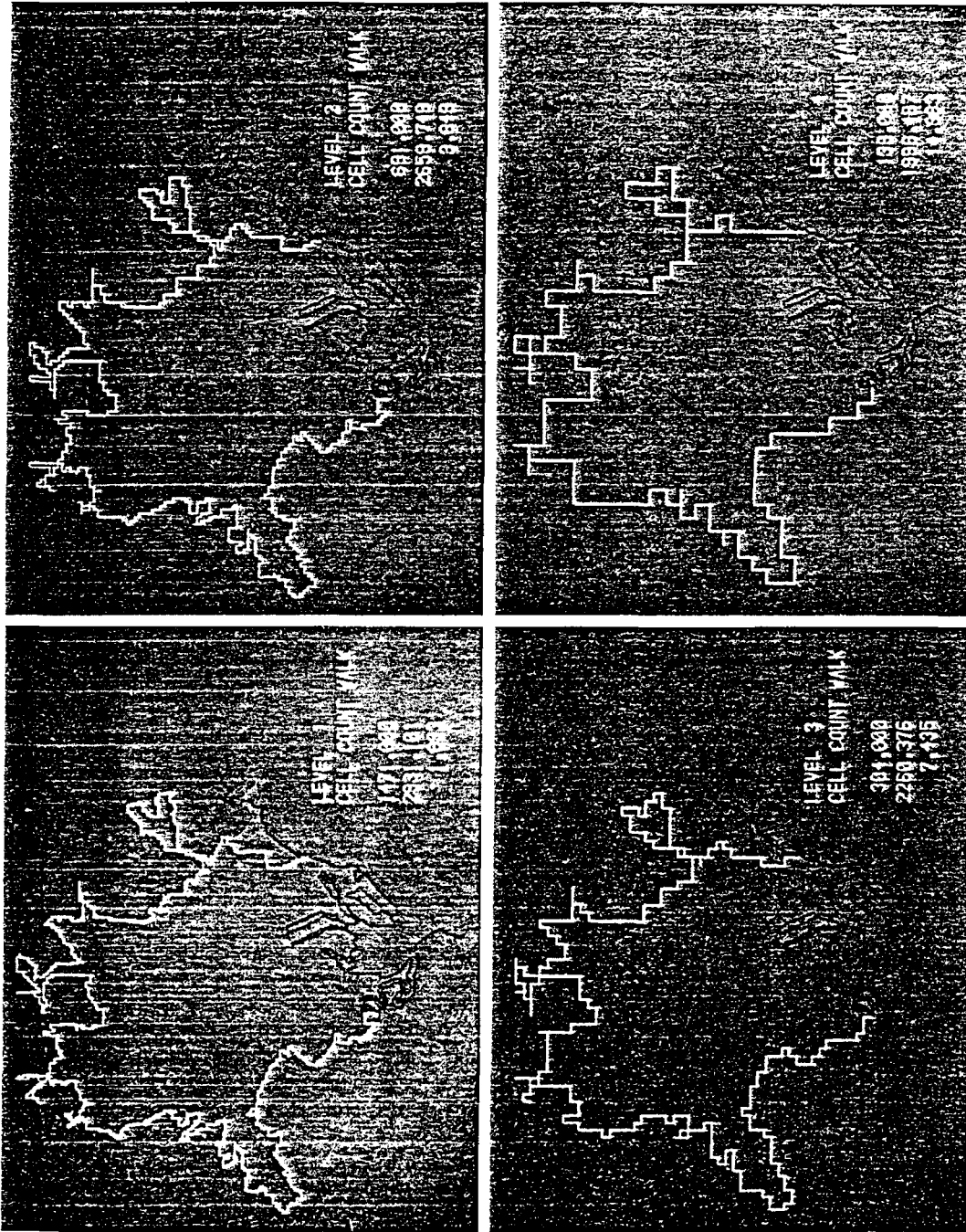


Figure 8. Illustration of cell-count procedure, using interactive computer graphics displays.

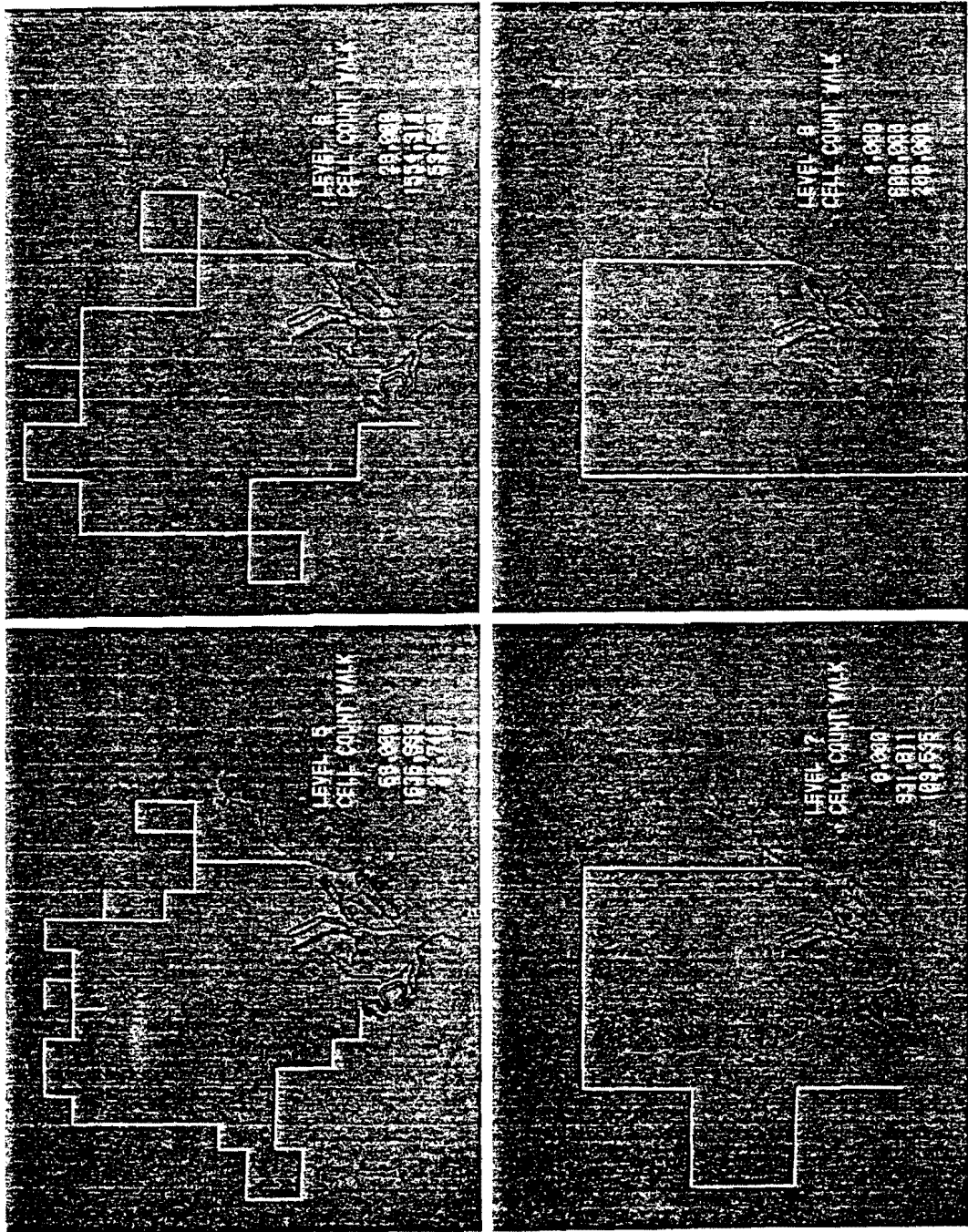


Figure 8. (Continued)

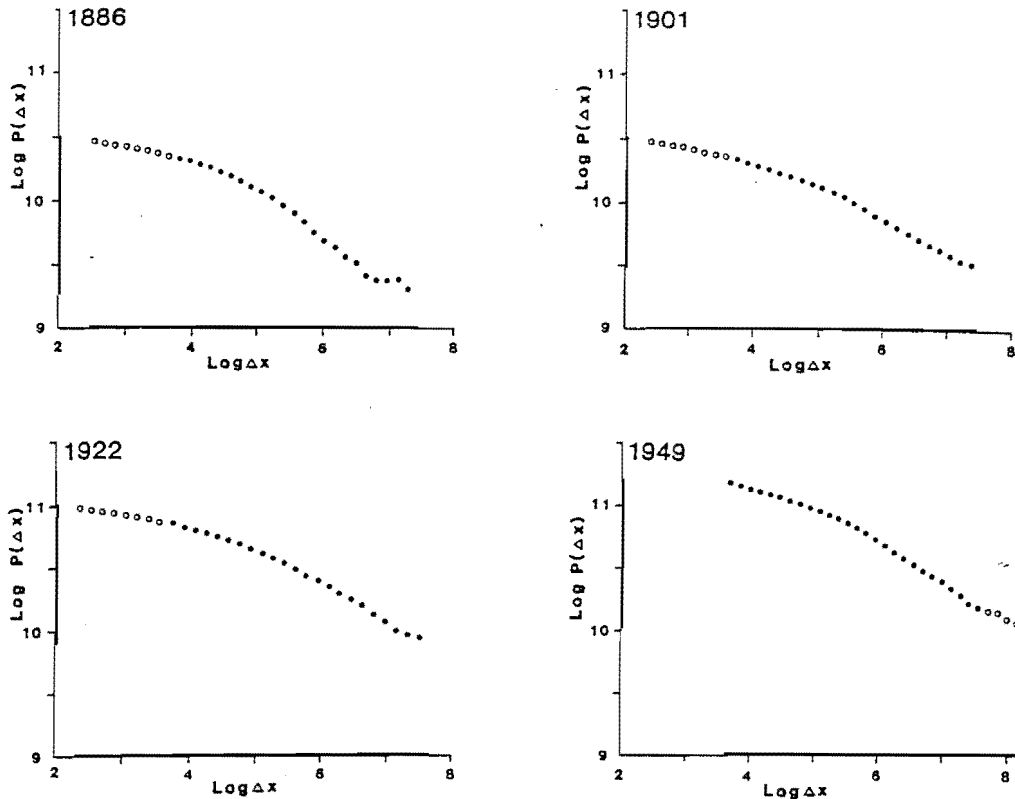


Figure 9. Richardson Plots of perimeter-scale relations for four time slices: cell count method.
 ● — Denotes observation falling within scale range common to all time slices.

endowed with different notions of distance (see Harvey, 1969, chap. 4, p. 191–229 for an explicitly geographical treatment). In the absence of map projections which permit an uncontentious interpretation of distance, there would seem to be an inevitable need to consider compound fractal dimensions.

This point brings the argument around full circle and requires us to make an explicit statement as to the relationship between measurement and theory. In short, is the notion of measurement useful beyond the simply descriptive if we are only to obtain complex

“black box” descriptors of cartographic phenomena which are the compound spatial expression of incompletely enumerated or incompletely understood processes? On this point Mandelbrot (1984) is unequivocal in his belief in the “absolute primacy of geometry over analytic refinement”; it is the role of subsequent theoretical development to disentangle the constituent “fractal eigendimensions” that may be of interest. Within the geographical literature, this sentiment is of continuing relevance in the context of Harvey’s (1969, p. 227) earlier concern that “the net-

Table 4. Cell count method: computational costs and statistical performances of competing functional forms

Date	CPU usage Days: hours: minutes	Log-Linear form (8)			Transient dimension model (12)			
		Log a	D	R ²	Log a	d*	b ₂ × 10 ⁻⁵	R ²
1886	3:04	11.326	1.267	0.953	11.109	1.207	3.525	0.973
1901	3:51	11.079	1.200	0.967	10.919	1.156	2.592	0.989
1922	11:30	11.617	1.209	0.957	11.426	1.156	2.686	0.988
1949	1:37	12.288	1.274	0.985	12.144	1.244	0.646	0.990

work for the interplay of formal mathematics and empirical problems is poorly connected". The prospect now may exist that through the wider involvement of computer cartographers and graphics analysts, we will identify the domain within which theoretical development can be informed most usefully by routinization of the measurement task.

REFERENCES

- Batty, M., 1985, Fractals — geometry between dimensions: *New Scientist*, v. 105, no. 1450, p. 31–35.
- Batty, M., and Longley, P., 1986, The fractal simulation of urban structure: *Environment and Planning A*, v. 18, no. 9, p. 1143–1179.
- Batty, M., and Longley, P.A., 1987, Fractal-based description of urban form: *Environment and Planning B*, v. 14, no. 2, p. 123–134.
- Bracken, I., 1985, Computer-aided cartography with microcomputers: a practical guide to MICROPLOT: Working Paper 90, Dept. Town Planning, UWIST, Cardiff, U.K., 78 p.
- Buttenfield, B., 1984, Line structure in graphic and cartographic space: Univ. Washington and University Microfilms International, Ann Arbor, Michigan, 320 p.
- Clark, N.N., 1986, Three techniques for implementing digital fractal analysis of particle shape: *Powder Technology*, v. 46, no. 1, p. 45–52.
- Daunton, M.J., 1977, *Coal Metropolis: Cardiff 1870–1914*: Leicester Univ. Press, Leicester, U.K., 260 p.
- Dearnley, R., 1985, Effects of resolution on the measurement of grain "size": *Mineralogical Magazine*, v. 49, no. 3, p. 539–546.
- Goodchild, M.F., 1980, Fractals and the accuracy of geographical measures: *Jour. Math. Geology*, v. 12, no. 1, p. 85–98.
- Goodchild, M., and Mark, D.M., 1987, The fractal nature of geographic phenomena: *Ann. Assoc. Am. Geographers*, v. 77, no. 2, p. 265–278.
- Harvey, D., 1969, *Explanation in geography*: Edward Arnold, London, 521 p.
- Kaye, B.H., 1978, Specification of the ruggedness and/or texture of a fine particle profile by its fractal dimension: *Powder Technology*, v. 21, no. 1, p. 1–16.
- Kaye, B.H., and Clark, G.G., 1985, Fractal dimension of extraterrestrial fineparticles: Dept. Physics, Laurentian Univ., Sudbury, Ontario, Canada, 16 p.
- Kaye, B.H., Leblanc, J.E., and Abbot, P., 1985, Fractal description of the structure of fresh and eroded aluminium shot fineparticles: *Particle Characterisation*, v. 2, no. 1, p. 56–61.
- Longley, P.A., and Batty, M., 1989, Measuring and simulating the structure and form of cartographic lines, in Hauer, J., Timmermans, H.J.P., and Wrigley, N., eds., *Contemporary developments in quantitative geography*: Reidel, Dordrecht, Holland, in press.
- Mandelbrot, B.B., 1984, Each fractal set has a unique fractal dimension, in Tatsumi, T., ed., *Turbulence and chaotic phenomena in fluids*: Elsevier, Amsterdam, p. 203–206.
- Morse, D.R., Lawton, J.H., Dodson, M.M., and Williamson, M.H., 1985, Fractal dimension of vegetation and the distribution of arthropod body lengths: *Nature*, v. 314, p. 731–733.
- Muller, J.-C., 1987, Fractal and automated line generalisation: *The Cartographic Jour.*, v. 24, no. 1, p. 27–34.
- Nakano, T., 1984, A systematics of "transient fractals" of rias coastline; an example of rias coast from Kamaishi to Shizugawa, northeastern Japan: *Ann. Rept., Inst. Geosci., Univ. Tsukuba*, no. 10, p. 66–68.
- Richardson, L.F., 1961, The problem of contiguity: an appendix to statistics of deadly quarrels: *General Systems Yearbook*, v. 6, no. 1, p. 139–187.
- Schertzer, D., and Lovejoy, S., 1984, On the dimension of atmospheric motions, in Tatsumi, T., ed., *Turbulence and chaotic phenomena in fluids*: Elsevier, Amsterdam, p. 505–512.
- Shelberg, M.C., Moellering, H., and Lam, N., 1982, Measuring the fractal dimensions of empirical cartographic curves: *Auto-Carto*, v. 5, p. 481–490.
- Wise, S., 1987, The use of fractals in thematic mappings: Working Paper, SWURCC, Univ. Bath, Bath, U.K., 12 p.